Progress In Electromagnetics Research C, Vol. 20, 227–238, 2011

A COMPACT PACKAGE WITH INTEGRATED PATCH ANTENNA FOR SINGLE-CHIP 60-GHZ RADIOS

L. L. Wai, K. M. Chua, and A. C. W. Lu

Singapore Institute of Manufacturing Technology
638075, Singapore

M. Sun and Y. P. Zhang

School of Electrical and Electronic Engineering
Nanyang Technological University, 639798, Singapore

Abstract—This paper presents the development of a standard surface mountable ceramic ball grid array (CBGA) package with an integrated patch antenna in low temperature cofired ceramic (LTCC) technology for emerging single-chip 60-GHz radios. It addresses the challenges of low-loss wire bonding interconnections required between the chip and the antenna as well as the package to allow efficient utilization of available space for miniaturization. The compact package of size $12.5\times8\times1.265\,\mathrm{mm}^3$ achieves good electrical performance. For instance, the package part exhibits insertion loss $< 0.08\,\mathrm{dB}$, return loss $> 22\,\mathrm{dB}$, and attenuation rate $< 0.2\,\mathrm{dB/cm}$ below 5 GHz; while the antenna part demonstrates 8-GHz impedance bandwidth and $8 \pm 2\,\mathrm{dBi}$ peak realized gain at 60 GHz. Simulated and measured results are compared. They agree reasonably well, indicating the feasibility of designing and manufacturing the integrated antenna package in LTCC for millimeter-wave applications.

1. INTRODUCTION

There is a growing interest today in low-power high-speed 60-GHz radios for a number of applications such as uncompressed high definition video streaming, mobile distributed computing, wireless gaming, Internet access, fast bulky file transfer, etc. [1]. These envisioned applications and potential huge market values have attracted both big companies and small start-ups to explore. For

Received 15 January 2011, Accepted 21 March 2011, Scheduled 25 March 2011
Corresponding author: Yue Ping Zhang (eypzhang@ntu.edu.sg).

example, IBM has demonstrated the 60-GHz fully integrated radio transmitter and receiver chipset in a 0.13-μm silicon-germanium (SiGe) technology [2] and Sibeam a 60-GHz transceiver chip in a 90-nm complementary metal oxide semiconductor (CMOS) technology [3].

With respect to the development of 60-GHz radio chipsets in silicon technologies, the development of packaging solutions to 60-GHz radio chipsets has also received attention. A land grid array (LGA) packaging solution for a 60-GHz radio chipset has been reported [4]. It adopts standard wire bonding except for the 60-GHz signal between the chip and the antenna. The antenna is a folded dipole constructed from a fused silica substrate, which is bonded to a metal frame using a thermosetting adhesive. The folded-dipole antenna achieves 7-dBi gain at 60 GHz and over 10% impedance bandwidth. A ball grid array (BGA) package together with a flip-chip attached 60-GHz transmitter or receiver IC has also been reported [5]. The packaged transmitter and receiver ICs, mounted on evaluation boards, have demonstrated beam-steered, non-line-of-sight links with data rates up to 5.3 Gb/s.

In this paper, we present the development of a standard surface mountable CBGA package with an integrated microstrip patch antenna in LTCC technology for emerging single-chip 60-GHz radios. The design considerations and fabrication details are described in Section 2. Simulated and measured results are discussed in Section 3. Finally, we conclude the paper in Section 4 with an outline of future developments.

2. PACKAGE CONCEPT

The integration of an antenna (or antennas) in a chip package relaxes the next-level subsystem interconnects as only low-frequency baseband or intermediate frequencies are conducted through the package pins while the high-frequency carrier signal is radiated from inside. It was originally proposed and demonstrated at frequencies below 6 GHz [6–10] and has been recently recognized as the most promising packaging solution to single-chip 60-GHz radios for low-power high-speed wireless communications [11–17].

2.1. Design Considerations

The design of a package needs to consider not only electrical, mechanical, and thermal issues but also manufacturable, testable, and assembly concerns. Figure 1 shows the top and bottom partially-transparent views of the package. As shown, the package features standard wire bonding. A three-tier cavity facilitates die mounting and efficient utilization of available space for signal routing and also to

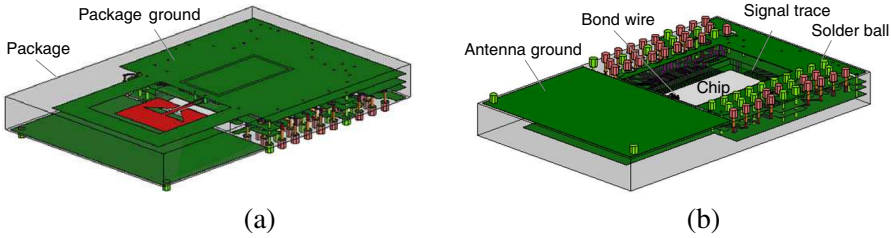

Figure 1. The package: (a) Top and (b) bottom partially-transparent views.

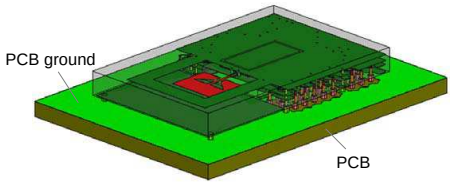

Figure 2. The package on the system PCB.

enable reduced parasitic from wire bonding. The radio die is adhered to the cavity base of the package ground plane. This configuration will contribute to the shielding of the radio die from the antenna [8]. The signals from the radio die are connected to the antenna through bond wires in a ground-signal-ground (G-S-G) configuration. The other signals from the radio die are connected to the outside system printed circuit board (PCB) by the bond wires, signal traces, vias, and solder balls. The ground planes in four layers are all connected by vias, and they are also connected to the outside system PCB by solder balls. The package has multiple input/outputs with a JEDEC standard solder ball pitch. Two dummy solder balls are attached to the two corners of the package, respectively for enhanced attachment on the system PCB as shown in Figure 2.

The antenna consists of a patch radiator [18, 19], a guard-ring director, and a ground-plane reflector. There is a slot cut on the patch radiator to have broader impedance bandwidth. The ground-plane reflector is introduced to make the radiator performance less sensitive to the system PCB-level dielectric and metal layers. The depth of the reflector is chosen to be $\lambda_g/4$ so that the radiation of the patch in free space can be enhanced by the reflector, where λ_g is the guided wavelength at 60 GHz. The guard-ring director plays an important role in this design and serves two purposes: first it helps to suppress the surface wave because $\lambda_g/2$ opened guard ring functions as an open

circuit to the surface wave, and second it helps to focus the radiation as a director. The coplanar waveguide (CPW) feed line is designed to be 50 Ω.

Bond wires are used in this package for interconnection. Bond wires between the radio die and the antenna is the most critical because the discontinuity introduced by bond wires can significantly affect the performance of the entire 60-GHz radio. Nonetheless, the wire-bonding technique, well established in consumer electronics, remains a very attractive solution since it is robust and inexpensive. In addition, it has the advantage of being tolerant on die and package thermal expansion, an important requirement for many applications. There are methods to compensate the discontinuity on either or both sides of the die and package for millimetre-wave applications [20, 21].

2.2. Fabrication Details

The package was fabricated in FERRO A6 LTCC ($\varepsilon_r = 5.9$ and $\tan\delta = 0.002$) with a panel size of $100 \times 100\,\text{mm}^2$ by LTCC Boutique Foundry in Singapore Institute of Manufacturing Technology.

Figure 3(a) shows the explored view of the package. Nine green (or un-fired) types were used to realize four cofired laminated ceramic layers for the package. The 1st ceramic layer is 0.385 mm thick; the 2nd ceramic layer is 0.285 mm thick with an opening $3.8 \times 2\,\text{mm}^2$; the 3rd

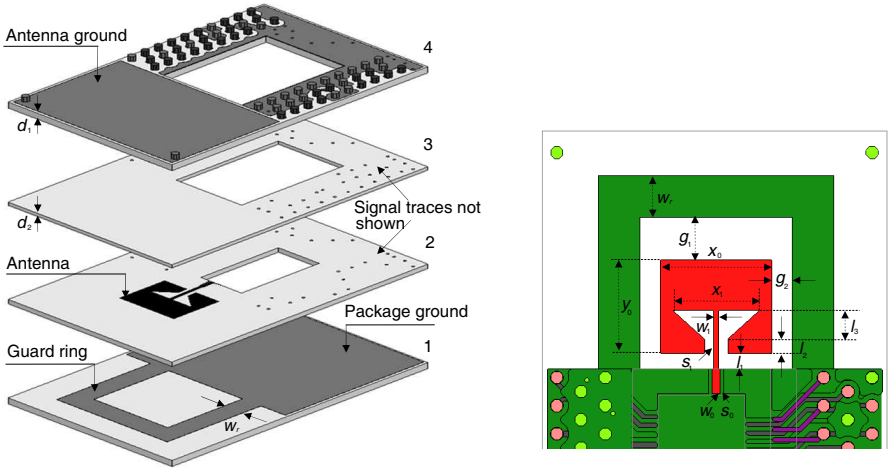

(a) (b)

Figure 3. (a) Explored view and (b) geometries and dimensions of the package.

layer is 0.21 mm thick with an opening $5 \times 3.2\,\text{mm}^2$; and the 4th layer is 0.385 mm thick with an opening $5 \times 3.8\,\text{mm}^2$. These openings form the three-tier cavity that can house the 60-GHz radio die of current size. There are also four metallic (gold) layers for the package. The top buried layer provides the metallization for the package ground plane and antenna guard ring, the 2nd buried layer the metallization for the patch radiator and signal traces, the 3rd buried layer the metallization for the signal traces, and the bottom exposed layer the metallization for the antenna ground plane and solder ball pads. The solder balls follow the JEDEC standard ball pitch of 0.65 mm. The antenna ground plane makes the antenna performance less sensitive to the system PCB-level dielectric and metal layers. The depth d of the antenna ground plane is chosen to be $d = d_1 + d_2 = 0.595\,\text{mm} \approx \lambda_g/4$ so that the radiation of the antenna in free space can be enhanced by the ground plane. Figure 3(b) also shows the detailed dimensions of the package. The size of the whole package is $12.5 \times 8 \times 1.265\,\text{mm}^3$. The dimensions of the patch antenna $w_0 = 0.18\,\text{mm}$, $s_0 = 0.09\,\text{mm}$, $g_1 = 0.99\,\text{mm}$, $g_2 = 0.48\,\text{mm}$, $w_1 = 0.12\,\text{mm}$, $s_1 = 0.21\,\text{mm}$, $l_1 = 0.36\,\text{mm}$, $l_2 = 0.33\,\text{mm}$, $l_3 = 0.66\,\text{mm}$, $x_0 = 2.58\,\text{mm}$, $y_0 = 2.16\,\text{mm}$, $x_1 = 2.01\,\text{mm}$. These values were obtained from the HFSS simulations and proved to be manufacturable by standard high-volume LTCC process [22].

Table 1 lists the wire bonding parameters. The wire profile or shape was designed based on the JEDEC standard. Note that the shortest bond wires are 300 µm long, which are for interconnection between the radio die and the antenna. The length of 300-µm is almost a doubled length of the shortest bond wire supported by the current technology and would thus greatly improve the yield of assembly of the chip with the package. Figure 4 shows the photo of the fabricated package.

Table 1. Wire bonding parameters.

Parameter	Value
Total length	0.3–0.5 mm
Diameter	0.025 mm
Die height	0.46 mm
Loop height	0.16 mm

3. RESULTS AND DISCUSSION

The fine features of the package require considerable computational power to simulate. Our available computer resource is insufficient, which forces us to simulate the package and antenna parts separately.

As most of the traces were buried in the 1st and 2nd tier cavity, embedded coplanar strips with ground plane topology was applied to the signal traces that require 50 ohm controlled impedance. Figure 5 shows the HFSS model in the design of the signal traces. It is evident that these signal traces involve bond wires, CPW lines, vias, and solder balls. The signal traces in purple, red, aqua, and blue are denoted as signal traces 1, 2, 3, and 4, respectively. Scattering parameter simulations were performed for a frequency range from 100 MHz to

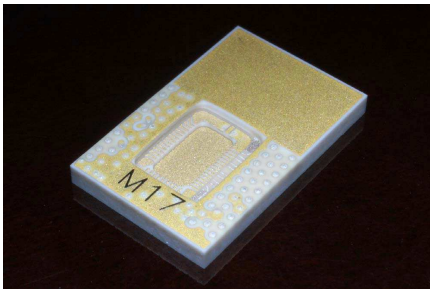

Figure 4. Photo of the package.

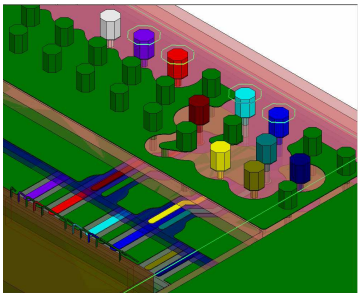

Figure 5. HFSS model of the signal traces that require 50 Ω controlled impedance of the package.

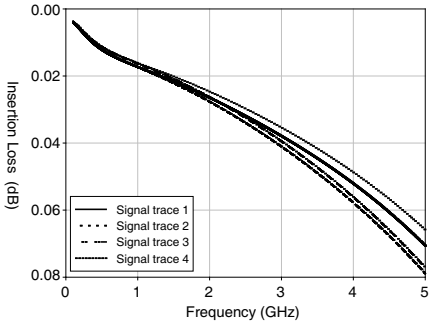

Figure 6. Insertion loss as a function of frequency.

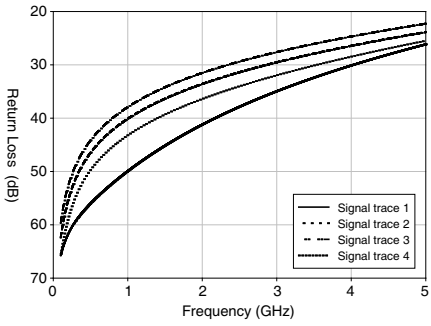

Figure 7. Return loss as a function of frequency.

5 GHz. Each signal trace end was connected to a 50-Ω port whilst ground traces were short-circuited to the ground plane, and each scattering parameter was obtained by exciting a single port whilst other ports were tied to 50-Ω match loads.

Figure 6 shows the simulated insertion loss characteristics from 100 MHz to 5 GHz for 50-Ω controlled impedance signal lines. It can be observed that the signal loss is very low up to 5 GHz, and the 3-dB insertion loss bandwidth is found to be much greater than 5 GHz, satisfying the 2-GHz bandwidth requirement easily.

Figure 7 shows the simulated return loss characteristics from 100 MHz to 5 GHz for 50-Ω controlled impedance signal lines. It is evident that a return loss of better than 22 dB is achieved over the 5-GHz bandwidth, indicating excellent wideband impedance matching to 50-Ω sources.

A transmission line parameter extraction methodology was also applied to obtain the frequency dependent parameter in terms of attenuation constant per unit length. Figure 8 indicates attenuation

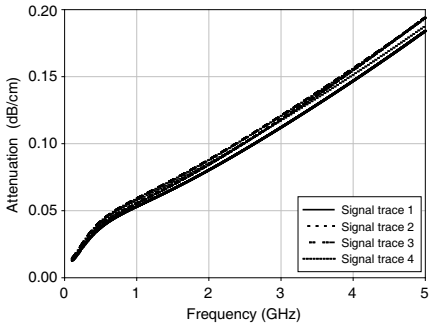

Figure 8. Attenuation as a function of frequency.

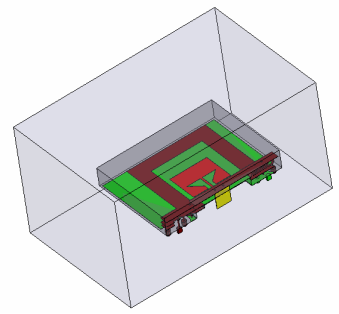

Figure 9. HFSS model of the antenna part of the package.

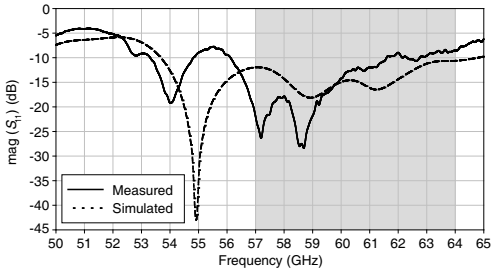

Figure 10. Simulated and measured input match $|S_{11}|$ profile.

characteristic of approximately 3.5 mm embedded coplanar strip transmission lines. It can be observed that maximum attenuation is only 0.2 dB/cm at 5 GHz.

Figure 9 shows the HFSS model of the antenna part with the wave-port excitation. The antenna function of the package was tested with a probe-based measurement setup at IBM Thomas J. Watson Research Center, USA. Due to equipment used, the measurement frequency is limited from 50 to 65 GHz, and only radiation patterns with 180° angular range can be obtained without setup change.

Figure 10 shows the input match $|S_{11}|$ of the antenna for a 50-Ω source. A good match from 56 to 66.5 GHz can be seen from the simulated $|S_{11}|$ profile, which even leaves some tolerance margin against the target bandwidth. An excellent match from 55.5 to 65 GHz can be seen from the measured $|S_{11}|$ profile, which clearly demonstrates that the antenna has a sufficient bandwidth for the 60-GHz radios [23].

Figure 11 shows the complex input impedance of the antenna. It is interesting to note from the measured impedance that the antenna exhibits capacitive reactance, which is actually quite desirable because

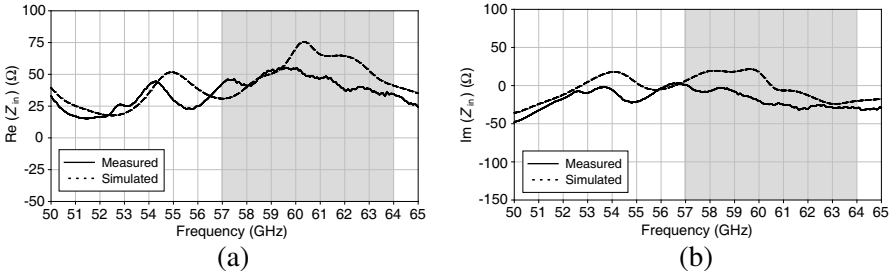

Figure 11. Simulated and measured complex input impedances of the antenna: (a) Real part and (b) imaginary part.

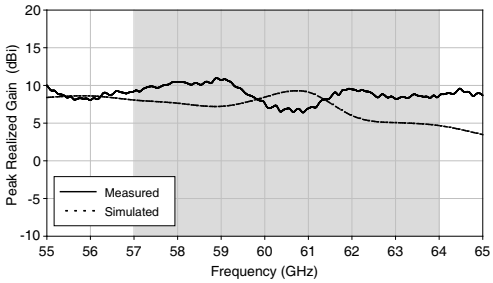

Figure 12. Simulated and measured gain of the antenna.

it makes easier to compensate the inductive reactance of the bond wires on the radio die side.

It should be noted that acceptable agreement has been achieved between the simulated and measured $|S_{11}|$ and impedance profiles. For example, there are three nulls at 55, 59, and 61.3 GHz in the simulated $|S_{11}|$ profile and at 54, 57.2, and 58.75 GHz in the measured $|S_{11}|$ profile, respectively. There are differences at the null locations and magnitudes, which are caused by the simplified HFSS model and the

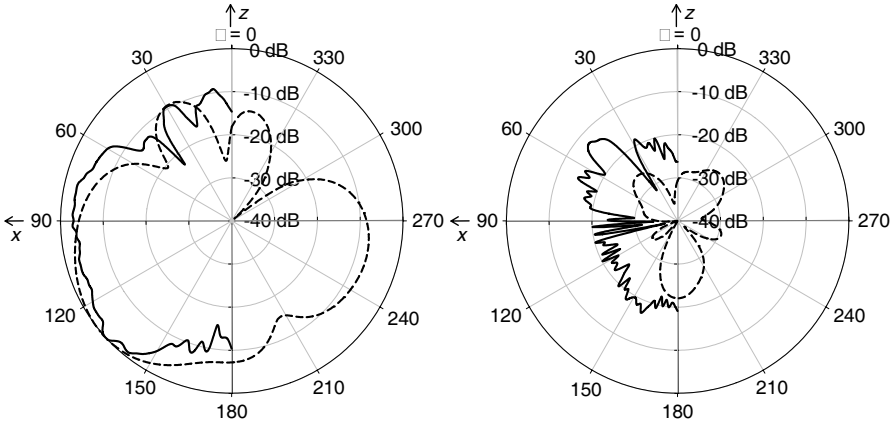

(a)

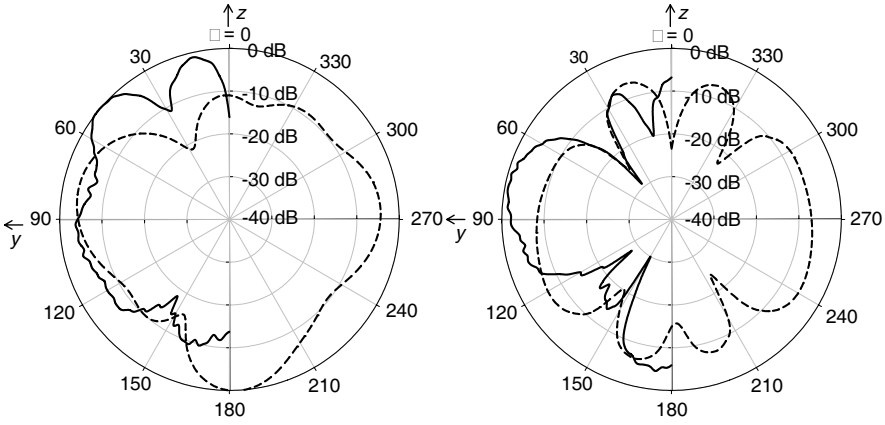

(b)

Figure 13. Simulated (dash line) and measured (solid line) radiation patterns of the AiP: (a) Patterns in the xz plane and (b) patterns in the yz plane.

misalignment of the wave-port excitation in simulations and the probe excitation in measurements.

Figure 12 shows the gain of the antenna over the frequency range from 55 to 65 GHz. It is seen that the measured and simulated peak realized gain values in the main beam direction vary 9 ± 2 dBi and 6 ± 2 dBi over the frequency range, respectively. The higher measured gain is due to the larger effective ground plane from the package part. The antenna efficiency was not measured but simulated to be more than 90% over the frequency range. The simulated high efficiency of the antenna should be true as the antenna is well matched, has higher measured gain, and exhibits comparable simulated and measured directivities. The high efficiency of the antenna is the result of the low-loss LTCC materials used and the surface waves suppressed.

Figure 13 shows the radiation patterns of the antenna at 61.5 GHz, respectively. The radiation patterns are different from those of a conventional patch antenna. A shaped-beam pattern can be seen in the co-polar xz-plane with the main beam in the directions from 120° to 150°. The shaped-beam pattern in the co-polar xz-plane is mainly caused by the grounded portion of the guard-ring director, which weakens the radiation of the antenna towards the die. The simulated radiation patterns agree reasonably well with the measured radiation patterns. The differences can be attributed to the fact that the simulation did not include the effect of the package part but the measurement did.

4. CONCLUSION

A compact package that integrated a guard-ring-directed, ground-plane-reflected, and CPW-fed patch antenna was designed, fabricated in LTCC, and experimentally verified for emerging single-chip 60-GHz radios. The careful design considerations simplified LTCC fabrication but still achieved excellent package and antenna performance. The package part exhibited insertion loss < 0.08 dB, return loss > 22 dB, and attenuation rate < 0.2 dB/cm below 5 GHz; while the antenna part demonstrated 8-GHz impedance bandwidth and 8 ± 2 dBi peak realized gain at 60 GHz.

As the current package integrated only one antenna element, the gain was not enough. It is therefore necessary to extend it to an array antenna to achieve higher gain. We are currently working on the design and realization of a package with an integrated array antenna in LTCC for 60-GHz applications. We believe that the antenna-in-package solution can be realized in other technologies such as liquid crystal polymer or at even higher frequency, say, 100 GHz. It is therefore

anticipated that the works presented in this paper are useful and inspiring for those interested in the development of highly-integrated mm-wave radios.

REFERENCES

1. http://www.ieee802.org/15/pub/TG3c.html.
2. http://domino.watson.ibm.com/comm/research_projects.nsf/pages/mmwave.sixtygig.html.
3. http://www.sibeam.com/.
4. Pfeiffer, U., J. Grzyp, D. Liu, B. Gaucher, T. Beukema, B. Floyd, and S. Reynolds, "A chip-scale packaging technology for 60-GHz wireless chipsets," *IEEE Trans. Microw. Theory Tech.*, Vol. 54, No. 8, 3387–3397, August 2006.
5. Kam, D. G., et al., "LTCC packages with embedded phased-array antennas for 60 GHz communications," *IEEE Microw. Wireless Compon. Lett.*, Vol. 21, No. 3, 142–144, March 2011.
6. Zhang, Y. P., T. K. C. Lo, and Y. Hwang, "A dielectric loaded miniature antenna for microcellular and personal communications," *Proc. of IEEE Antenna Propagat. Symp.*, 1152–1155, Newport Beach, California, USA, June 18–23, 1995.
7. Zhang, Y. P., "Integration of microstrip antenna on cavity-down ceramic ball grid array package," *Electronics Lett.*, Vol. 38, No. 22, 1307–1308, October 2002.
8. Ryckaert, J., et al., "Single-package 5 GHz WLAN RF module with embedded patch antenna and 20 dBm power amplifier," *Digest of IEEE MTT-S Int. Symp.*, 1037–1040, 2003.
9. Zhang, Y. P., "Integrated ceramic ball grid array package antenna," *IEEE Trans Antennas Propagat.*, Vol. 52, No. 10, 2538–2544, October 2004.
10. Wi, S. H., et al., "Package-level integrated antennas based on LTCC technology," *IEEE Trans. Antennas Propagat.*, Vol. 54, No. 8, 2190–2197, 2006.
11. Tsutsumi, Y., et al., "A triangular loop antenna mounted adjacent to a lossy Si substrate for millimeter-wave wireless PAN," *Proc. of IEEE Antenna Propagat. Symp.*, 1008–1011, Honolulu, Hawaii, USA, June 10–15, 2007.
12. Zhang, Y. P., M. Sun, K. M. Chua, L. L. Wai, and D. Liu, "Integration of slot antenna in LTCC package for 60-GHz radios," *Electronics Lett.*, Vol. 44, No. 5, 330–331, March 2008.
13. Yoshida, S., K. Tsubouchi, A. Tosaki, H. Oguma, S. Kameda,

H. Nakase, and T. Takagi, "Radiation characteristics of ultra-small wireless communication modules for 60 GHz band WPAN," *Proc. IEEE Antenna Propagat. Symp.*, San Diego, California, USA, July 5–12, 2008.

14. Sun, M., Y. P. Zhang, K. M. Chua, L. L. Wai, D. X. Liu, and B. Gaucher, "Integration of Yagi antenna in LTCC package for differential 60-GHz radio," *IEEE Trans. Antennas Propagat.*, Vol. 56, No. 8, 2780–2783, August 2008.
15. Zhang, Y. P., M. Sun, K. M. Chua, L. L. Wai, and D. Liu, "Antenna-in-package design for wirebond interconnection to highly-integrated 60-GHz radios," *IEEE Trans. Antennas Propagat.*, Vol. 57, No. 10, 2842–2852, October 2009.
16. Zhang, Y. P. and D. Liu, "Antenna-on-chip and antenna-in-package solutions to highly-integrated millimeter-wave devices for wireless communications," *IEEE Trans. Antennas Propagat.*, Vol. 57, No. 10, 2830–2841, October 2009.
17. Sun, M., Y. P. Zhang, Y. X. Guo, K. M. Chua, and L. L. Wai, "Integration of grid array antenna in chip package for highly integrated 60-GHz radios," *IEEE Antennas Wireless Propagat. Lett.*, Vol. 8, 1364–1366, 2009.
18. Kasabegoudar, V. G. and K. J. Vinoy, "A broadband suspended microstrip antenna for circular polarization," *Progress In Electromagnetics Research*, Vol. 90, 353–368, 2009.
19. Islam, M. T., M. N. Shakib, and N. Misran, "Design analysis of high gain wideband L-probe FED microstrip patch antenna," *Progress In Electromagnetics Research*, Vol. 95, 397–407, 2009.
20. Budka, T. P., "Wide-bandwidth millimeter-wave bond-wire interconnects," *IEEE Trans. Microw. Theory Tech.*, Vol. 49, No. 4, 715–718, April 2001.
21. Sun, Y., S. Glisic, F. Herzel, K. Schmalz, E. Grass, W. Winkler, and R. Kraemer, "An integrated 60 GHz transceiver front end for OFDM in SiGe: BiCMOS," *Wireless World Research Forum 16*, Shanghai, China, April 26–28, 2006.
22. Wang, Z., P. Li, R.-M. Xu, and W. Lin, "A compact X-band receiver front-end module based on low temperature co-fired ceramic technology," *Progress In Electromagnetics Research*, Vol. 92, 167–180, 2009.
23. Shireen, R., S. Shi, and D. W. Prather, "Wideband millimeter-wave bow-tie antenna," *Journal of Electromagnetic Waves and Applications*, Vol. 23, Nos. 5–6, 737–746, 2009.